UNIVERSITY OF NIŠ
The scientific journal "FACTA UNIVERSITATIS"
Series: "Physics, Chemistry and Technology" Vol.1, N° 2, 1995. 143-159
Editor of Series: Predrag Dimitrijević
Address: Trg bratstva i jedinstva 2 YU-18000 Niš
Tel: +381 18 23953 Fax: +381 18 24488

WAVE DAMPING INFLUENCE ON STIMULATED RAMAN SCATTERING BEHAVIOUR IN A HOMOGENEOUS PLASMA

M.S. Jovanović*
M.M. Škorić**

* *Department of Physics, University of Niš, P.O. BOX 91, 18001 Niš, Yugoslavia*
** *Vinča Institute of Nuclear Sciences, P.O. BOX 522, 11001 Belgrade, Yugoslavia*

Abstract: A problem of (non)stationarity of nonlinearly saturated regime of stimulated Raman backscattering in a homogeneous plasma layer is examined. Slowly varying wave envelope equations with the damping and the nonlinear frequency shift terms included are treated numerically and analytically. It is demonstrated that the variation in the damping rate drives the system through various dynamical regimes (from the steady–state to the chaotic one). Quantitative relations that enable prediction of the type of asymptotic (saturated) behaviour of Raman instability are obtained and discussed.

1. Introduction

Recent experimental observations and theoretical considerations have revealed that the process of stimulated Raman scattering (SRS) [1,2], being relatively fast with respect to the pump laser pulse duration, can attain a nonlinear saturation [2,3], which is indicated by anomalous reflection of the laser light. Namely , the SRS–induced (daughter) backscattered transverse and electron plasma waves (EPW) grow from the noise level until limited by the arrival at the boundaries of the plasma or by nonlinear effects, such as pump depletion or any other type of wave nonlinearities [4–7], one of which is concerned in the present paper. The time–asymptotic saturated regime is either purely stationary (steady–state), which assumes wave amplitudes constant in time, or, alternatively, the evolution can express features of periodic or aperiodic, irregular temporal behaviour. Both types of saturated behaviour are encountered, judging by different backscattering spectra observed in recent experiments [8–10] and simulations [11]. The kind of asymptotic state realized clearly depends on the values of physical parameters applied in an experiment or a numerical simulation. This question is going to be examined in more detail in this paper.

Numerous parameters of the system laser–plasma play a significant role in determining the direction of SRS nonlinear saturation. The emphasis will be put here on the influence that the linear damping of EPW's has on the type of the saturation of stimulated Raman *back*scattering (SRBS) in a finite homogeneous plasma, regardless of the origin of the damping (Landau mechanism, electron–ion collisions etc.). Our analysis is based on the numerical simulation of the system of three coupled nonlinear first–order partial differential

UDK: 533.9.01; Received 6. August 1995.

equation, governing the space–time development of the pump, backscatter and EPW. In this paper, we examine the critical point, corresponding to the conditions under which the system transits from stationary to a nonstationary asymptotic state.

The novelty in relation to the previous papers dealing with similar topics [4,6,7] is an inclusion of the nonlinear frequency shift (NLFS) in the equation corresponding to the SRS–driven EPW. This nonlinearity is due either to a ponderomotive coupling to low–frequency ion modes [5,6,12] or to a relativistic detuning caused by the relativistic mass correction [13], which is a well–known effect in the studies of large amplitude plasma waves. For instance, this effect is responsible for the wave saturation in a beat–wave accelerator. The NLFS can also cause the modulational instability of the wave, which leads eventually to spectrum broadening and the development of spatio–temporal chaos, as demonstrated recently by these authors [14].

In Section 2., the partial differential equations governing the space–time evolution of the waves taking part in the SRS process are introduced. Their convenient normalization is presented, and basic parameters determining the process behaviour are listed.

Section 3. presents the results of numerical simulation of the SRBS equations for the cases of a moderate and a strong pumping and for different values of linear EPW damping rate. Transitions from stationary to a nonstationary backscatter dynamics is observed when varying the damping coefficient.

An analytic approach presented in Section 4. starts from stationary solutions for wave amplitudes and considers their stability to small perturbations. The equations are derived that connect the critical parameters corresponding to the transition between stationary and nonstationary SRBS, and the appropriate bifurcation diagram is plotted.

2. Basic theory

According to the standard procedure, basic fluid and Maxwell equations are combined to give three coupled wave equations which govern the evolution of each wave amplitude. Since these equations have been derived in many references concerning nonlinear three–wave interactions [2,15], although perhaps presented in different forms, we will omit an elementary procedure and forward to the final set of coupled wave equations describing the one–dimensional interaction, namely SRBS influenced by intense laser radiation in a finite, homogeneous, fully ionized plasma with one species of fixed ions:

$$\frac{\partial E_0}{\partial t} + v_0 \frac{\partial E_0}{\partial x} + \nu_0 E_0 + i\sigma_0 |E_0|^2 E_0 = i \frac{\omega_{pe}^2}{4 n_0 \omega_1} E_1 \delta n_e, \tag{1a}$$

$$\frac{\partial E_1}{\partial t} + v_1 \frac{\partial E_1}{\partial x} + \nu_1 E_1 + i\sigma_1 |E_1|^2 E_1 = i \frac{\omega_{pe}^2}{4 n_0 \omega_0} E_0 \delta n_e^*, \tag{1b}$$

$$\frac{\partial \delta n_e}{\partial t} + v_2 \frac{\partial \delta n_e}{\partial x} + \nu_2 \delta n_e + i\sigma_2 |\delta n_e|^2 \delta n_e = i \frac{\varepsilon_0 \omega_{pe}^2 k_2^2}{4 m_e \omega_0 \omega_1 \omega_2} E_0 E_1^*, \tag{1c}$$

where $E_0(x,t)$ and $E_1(x,t)$ are the electric field amplitudes of the pump and backscattered waves, respectively, and $\delta n_e(x,t)$ is EPW–induced electron density fluctuation. The group velocities of the three interacting waves are calculated according to:

$$v_0 = \frac{c^2 k_0}{\omega_0}, \quad v_1 = \frac{c^2 k_1}{\omega_1}, \quad v_2 = \frac{3 k_2 v_T^2}{\omega_2}, \tag{2}$$

and the wave damping rates:

$$\nu_0 = \frac{\omega_{pe}^2 \nu_{ei}}{2\omega_0^2}, \quad \nu_1 = \frac{\omega_{pe}^2 \nu_{ei}}{2\omega_1^2}, \quad \nu_2 = \frac{\nu_{ei} + \Gamma}{2} \tag{3}$$

In the expressions (1)–(3), the following notation was used: ω_{pe} is the electron plasma frequency, n_0 — equilibrium electron or ion density, v_T — electron thermal velocity $\left(v_T = \sqrt{\kappa T_e / m_e}\right)$, ε_0 — dielectric constant of vacuum, ν_{ei} — electron–ion collisional frequency and Γ — a contribution to the damping rate by other dissipative effects (Landau damping, in the first place). Perfect matching conditions for the frequencies and wave numbers are assumed here:

$$\omega_0 = \omega_1 + \omega_2, \quad k_0 = -k_1 + k_2. \tag{4}$$

Two remarks deserve more attention at this point. The system of nonlinear partial differential equations (1), which is of the first order in space and time derivatives, is derived from the second–order system by multiple scale procedure, which assumes that every wave–connected function is separated into its slow and fast parts:

$$f(x,t) \to \overline{f}(x,t)\, \mathrm{e}^{\mathrm{i}(\omega_j t - k_j x)}, \tag{5}$$

where $\overline{f}$ is a slowly–varying (in space and time) envelope of a function f, indices $j = 0, 1, 2$ being associated with the pump, backscattered and plasma waves, respectively. The approximation given by (5) is justified provided any spatial and temporal growths resulting from the nonlinear coupling occur on a scale long compared to one wavelength or to one period of oscillations. This important condition will we keep in mind considering a spatio–temporal development of the wave amplitudes.

Another characteristic of the system (1) is the inclusion of self–modal cubic nonlinear terms. These terms have the form of the NLFS, and they, as stressed in the Introduction, originate from possible nonlinear phase detuning in large amplitude fields [12,16]. The coefficients σ_i are phenomenological constants, whose values depend on the effect the nonlinearity is generated from. Powerful lasers that are used in nowadays experiments excite high–intensity waves, so that many wave nonlinearities appear to be relevant [6,12,16]. This relates, in particular, to EPW's, and the physics of large amplitude plasma waves is under intensive study of the plasma physicists at the moment. Therefore, we shall retain the damping and the NLFS terms only in the EPW equation (1c), assuming the latter effect originating from ponderomotive effects [12]:

$$\sigma_2 = \frac{1}{8} \frac{\omega_{pe}^2}{n_0^2 v_T^2 k_2^2}, \tag{6a}$$

or the relativistic correction of electron mass [13,17]:

$$\sigma_2 = \frac{3}{16} \frac{\omega_{pe}^2}{c^2 n_0^2 k_2^2}. \tag{6b}$$

As will be seen in the forthcoming text, this nonlinearity has a crucial effect on the asymptotic SRS behaviour, once the amplitude of the EPW becomes comparable to those of the other two waves.

Before proceeding with the analysis of the coupled equations, it is useful to introduce normalized amplitudes of the waves involved:

$$a_0(x,t) = \frac{E_0(x,t)}{\mathcal{E}_0}, \quad a_1(x,t) = \frac{E_1(x,t)}{\mathcal{E}_0}, \quad a_2(x,t) = -i\,\frac{\delta n_e(x,t)}{n_0}, \tag{7}$$

where $\mathcal{E}_0$ designates the incident amplitude of the pump wave $(\mathcal{E}_0 \equiv E_0(0,t))$. In this way the coupled system (1) takes the form:

$$\frac{\partial a_0}{\partial t} + v_0\frac{\partial a_0}{\partial x} = -\Omega_0 a_1 a_2, \tag{8a}$$

$$\frac{\partial a_1}{\partial t} - v_1\frac{\partial a_1}{\partial x} = \Omega_1 a_0 a_2^*, \tag{8b}$$

$$\frac{\partial a_2}{\partial t} + v_2\frac{\partial a_2}{\partial x} + \frac{\Gamma}{2}a_2 + i\sigma|a_2|^2 a_2 = \Omega_2 a_0 a_1^*, \tag{8c}$$

where

$$\Omega_0 = \frac{\omega_{pe}^2}{4\omega_1}, \quad \Omega_1 = \frac{\omega_{pe}^2}{4\omega_0}, \quad \Omega_2 = \frac{\varepsilon_0\omega_{pe}^2 k_2^2 \mathcal{E}_0^2}{4m_e n_0\omega_0\omega_1\omega_2}. \tag{9}$$

The frequencies and the wave numbers of all waves are determined once the pump wave frequency ω_0 is set. Namely, the matching conditions (4), together with the well–known dispersion relations of electromagnetic and EPW's, produce the following:

$$k_0 = \frac{\omega_0}{c}\sqrt{1-\alpha^2}, \tag{10}$$

$$\omega_1 = \omega_0(1-\alpha)\left[1 - \frac{3}{2}\frac{v_T^2}{c^2}\frac{\left(\sqrt{1-\alpha^2}+\sqrt{1-2\alpha}\right)^2}{\alpha(1-\alpha)}\right], \tag{11a}$$

$$k_1 = \frac{\omega_0}{c}\sqrt{1-2\alpha}\left[1 - \frac{3}{2}\frac{v_T^2}{c^2}\frac{(1-\alpha)\left(\sqrt{1-\alpha^2}+\sqrt{1-2\alpha}\right)^2}{\alpha\sqrt{1-2\alpha}}\right], \tag{11b}$$

$$\omega_2 = \omega_0\alpha\left[1 + \frac{3}{2}\frac{v_T^2}{c^2}\frac{\left(\sqrt{1-\alpha^2}+\sqrt{1-2\alpha}\right)^2}{\alpha^2}\right], \tag{12a}$$

$$k_2 = \omega_0(1-\alpha)\left[1 - \frac{3}{2}\frac{v_T^2}{c^2}\frac{\left(\sqrt{1-\alpha^2}+\sqrt{1-2\alpha}\right)^2}{\alpha(1-\alpha)}\right], \tag{12b}$$

where the terms containing the temperature factor (v_T/c) are considered small corrections to the fundamental (cold plasma limit) values, and

$$\alpha = \frac{\omega_{pe}}{\omega_0} = \sqrt{\frac{n_0}{n_{cr}}}, \tag{13}$$

n_{cr} designating the density on the critical surface, where electron plasma frequency ω_{pe} equals the pump wave frequency ω_0.

If we neglect the finite temperature correction in the expressions (10)–(12), the constant coefficients in the equations (8) can be written in terms of dimensionless parameters as follows:

$$v_0 = \sqrt{1-\alpha^2}\,c, \quad v_1 = \frac{\sqrt{1-2\alpha}}{1-\alpha}\,c, \quad v_2 = \frac{3\frac{v_T^2}{c^2}\left(\sqrt{1-\alpha^2}+\sqrt{1-2\alpha}\right)}{\alpha}\,c, \tag{14}$$

$$\Omega_0 = \frac{\alpha^2}{4(1-\alpha)}\,\omega_0, \quad \Omega_1 = \frac{\alpha^2}{4}\,\omega_0, \quad \Omega_2 = \frac{\beta_0^2\left(\sqrt{1-\alpha^2}+\sqrt{1-2\alpha}\right)}{4\alpha(1-\alpha)}\,\omega_0. \tag{15}$$

The quantity β_0, appearing in the last expression, refers to a relative pump strength, i.e. the ratio between the electron quiver velocity in the incident laser field of v_{osc} and the speed of light in vacuum:

$$\beta_0 = \frac{v_{osc}}{c} = \frac{e\mathcal{E}_0}{m_e\omega_0 c}, \tag{16}$$

which can be expressed in terms of the incident wave intensity I and wavelength λ_0 [18]:

$$\beta_0 = 8.53\times 10^{-10}\sqrt{I\,[W/cm^2]}\;\lambda_0[\mu m]. \tag{17}$$

As for the NLFS coefficient σ, it can take different values, depending on its generics, and we shall adopt the constant value $\sigma = 0.01\omega_{pe}$ in all our simulations.

3. Results of simulation

When studying numerically the SRS instability in a finite homogeneous plasma layer by means of the system of differential equations (8), several parameters make effect on the temporal development of reflectivity, fraction and the temporal dependence of the backscattered towards the laser pump energy. The most important among them are: pump intensity I, pump wavelength λ_0, plasma length L, electron density n_e and temperature T_e and EPW damping rate Γ. Some of these parameters will we keep fixed in numerical simulations: $n_e = 0.1\,n_{cr}$, $L = 100\,c/\omega_0$, $\kappa T_e = 1\,keV$. Note that these values appear typical for a class of experiments with preformed or fusion plasmas [1,19]. The pump intensity is most to a large variation in experiments. The β_0 parameter lies, usually, in the interval 10^{-3}–10^{-1}. Thus, we applied two trial values of β_0: 0.03 and 0.1. The EPW damping rate Γ is most obscure of all parameters listed above. Its value is frequently beyond experimentalists' control, so we made a series of numerical calculations for diverse values of its magnitude.

The most usually observed quantitative feature of the Raman instability to experimentalists as well as to theorists is backscattered intensity, which we will observe through the SRS reflectivity R — the fraction of the incident intensity, reflected in the backscattering process, towards the pump radiation intensity:

$$R = \frac{I_1}{I_0} = \frac{v_1|E_1(0,t)|^2}{v_0|E_0(0,t)|^2} = \frac{v_1}{v_0}|a_1(0,t)|^2 = \frac{\sqrt{1-2\alpha}}{(1-\alpha)\sqrt{1-\alpha^2}}|a_1(0,t)|^2, \tag{18}$$

which, in principle, can be a function of time in a nonstationary regime of nonlinear saturation.

In order to start with a numerical simulation of the partial differential equations (8), certain initial and boundary conditions are needed. We input here nonzero source boundary conditions, which assume a finite starting noise level for the backscattered electromagnetic waves:

$$\begin{aligned} &E_0(x,0) = 0 \Rightarrow a_0(x,0) = 0, \\ &E_0(0,t) = \mathcal{E}_0 \Rightarrow a_0(0,t) = 1, \\ &E_1(x,0) = E_1(L,t) = \varepsilon\mathcal{E}_0 \Rightarrow a_1(x,0) = a_1(L,t) = \varepsilon, \\ &\delta n_e(x,0) = \delta n_e(0,t) = 0 \Rightarrow a_2(x,0) = a_2(0,t) = 0. \end{aligned} \tag{19}$$

where the value $\varepsilon = 10^{-3}$ is taken for the noise level.

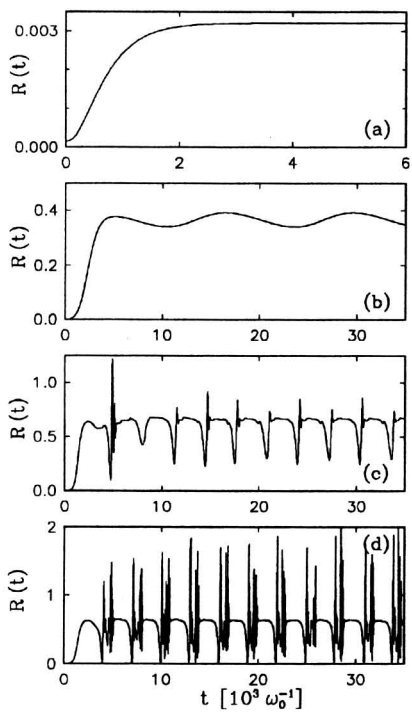

Fig. 1. Temporal development of SRBS reflectivity in a homogeneous plasma layer for: β_0=0.03, n_e=0.1n_{cr}, L=100c/ω_0, κT_e=1keV, ε_0=10^{-3}, and for EPW damping rates Γ/ω_{pe}: a) 2×10^{-2}, b) 10^{-3}, c) 10^{-4}, d) 10^{-5}.

The first series of simulations was performed with a moderate value of the pump strength: $\beta_0 = 0.03$. When the EPW damping was as strong as $\Gamma = 2 \times 10^{-2}\omega_{pe}$ (Fig. 1a), the system tended to a fully saturated steady state with a rather small reflectivity, which is amortized by the action of strong damping. When decreasing the damping rate, the system bifurcates at some critical point to a nonstationary regime, which is at first purely periodic (oscillatory) (Fig. 1b, for $\Gamma = 10^{-3}\omega_{pe}$). Then, the system transits to states with

ever less regularity in its temporal evolution. Thus, Figs. 1c and 1.d (for $\Gamma = 10^{-4}\omega_{pe}$ and $\Gamma = 10^{-5}\omega_{pe}$, respectively) show the regimes that are referred to as intermittent in the nonlinear dynamics theory [20]. The term temporal intermittency refers to a dynamical regime which alternates in time between regular evolution periods and spells of chaotic burst appearances.

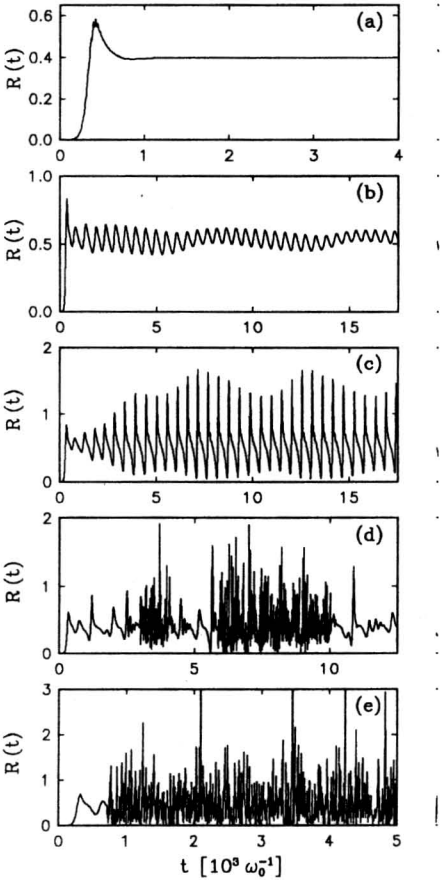

Fig. 2. Temporal development of SRBS reflectivity in a homogeneous plasma layer for: β_0=0.1, n_e=0.1n_{cr}, L=100c/ω_0, κT_e=1keV, ε_0=10^{-3}, and for EPW damping rates Γ/ω_{pe}: a) 0.06, b) 0.02, c) 0.018, d) 0.012, e) $10^{-5}\omega_{pe}$.

The transition between different dynamical regimes is even more visible in the case of a strong pump, for instance $\beta_0 = 0.1$ (Fig. 2). The first diagrams in Fig. 2 correspond, approximately, to those presented in Fig. 1. What is new and more interesting in this figure is the appearance of a full chaoticity in the reflectivity evolution, as seen in the Fig. 2e, which shows the case of relatively weak, practically negligible damping ($\Gamma = 10^{-5}\omega_{pe}$).

This chaotic regime in SRBS is examined in more details elsewhere [21,22]. What is in our focus here are the conditions of transition of SRS between stationary (steady–state) and nonstationary regimes, to which the forthcoming section of the present paper is devoted.

4. Onset of the nonstationary SRBS

The aim of the present section is determination of critical conditions under which the system exhibiting nonlinearly saturated SRBS in the steady state (with constant reflectivity R) transits to a regime with R changing its value in the course of time. Let us start from ordinary differential equations, following from the system (8), which describe the spatial dependence of the coupled wave amplitudes in the stationary SRBS regime:

$$v_0 A_0' = -\Omega_0 A_1 A_2, \tag{20a}$$

$$v_1 A_1' = -\Omega_1 A_0 A_2^*, \tag{20b}$$

$$v_2 A_2' + \frac{\Gamma}{2} A_2 + i\sigma |A_2|^2 A_2 = \Omega_2 A_0 A_1^*, \tag{20c}$$

where the apostrophes stand for derivatives in x. The convective term in the equation (20c) can be assumed non–dominant for here applied parameters (v_0=0.95c, v_1=0.87c, v_2=0.029c). As we concern the damping effects, which are important at high Γ, we shall drop the spatial derivative term in (20c) and adopt this equation in the form:

$$\left(\frac{\Gamma}{2} + i\sigma |A_2|^2\right) A_2 = \Omega_2 A_0 A_1^*. \tag{21}$$

Thus, the set of equations (20) is reduced to a system containing two differential and one algebraic equation. According to (19), the following boundary conditions are to be obeyed by the waves A_0 and A_1:

$$A_0(0) = 1, \quad A_1(L) = \varepsilon. \tag{22}$$

Once the stationary state, given by equations (20a), (20b) and (21), is established, it will be stable only if fluctuations (or small perturbations) imposed to the wave amplitudes are damped in time. Therefore, in the vicinity of the nonstationarity threshold, we can express perturbed amplitude solutions in the form:

$$a_i(x,t) = A_i(x) + \delta a_i(x) \exp(\gamma t), \qquad (i = 0,1,2) \tag{23}$$

where δa_i's are perturbation functions, and γ is instability increment (or decrement), whose sign tells us about the stationary solution stability (the case $\gamma > 0$ corresponds to the appearance of nonstationarity).

Substituting (23) into equations (8), and taking into account stationary equations (20), we arrive to the system of ordinary differential equations governing the spatial dependence of δa_i:

$$\begin{aligned}
\gamma \delta a_0 + v_0 \frac{d\delta a_0}{dx} &= -\Omega_0 (A_1 \delta a_2 + A_2 \delta a_1), \\
\gamma \delta a_1 - v_1 \frac{d\delta a_1}{dx} &= \Omega_1 (A_0 \delta a_2^* + A_2^* \delta a_0), \\
\gamma \delta a_2 - v_2 \frac{d\delta a_2}{dx} &+ \left(\frac{\Gamma}{2} + i\sigma |A_2|^2\right) \delta a_2 = \Omega_2 (A_0 \delta a_1^* + A_1^* \delta a_0),
\end{aligned} \tag{24}$$

which are supposed to fulfill the following boundary conditions:

$$\delta a_0(0) = \delta a_1(L) = \delta a_2(0) = 0, \tag{25}$$

following from the conditions (19) and (22). As in earlier evaluations, we omit the convection term in the third of equations (24). In order to simplify the analysis and keeping in mind the boundary conditions (25), we approximate now:

$$\frac{d\delta a_0}{dx} \approx \frac{\delta a_0}{L}, \quad \frac{d\delta a_1}{dx} \approx -\frac{\delta a_1}{L}. \tag{26}$$

Thus, the system of ordinary differential equations (24) reduces to a system of six homogeneous algebraic equations:

$$\begin{pmatrix} \gamma+\frac{v_0}{L} & 0 & \Omega_0 A_2 & 0 & \Omega_0 A_1 & 0 \\ 0 & \gamma^*+\frac{v_0}{L} & 0 & \Omega_0 A_2^* & 0 & \Omega_0 A_1^* \\ -\Omega_1 A_2^* & 0 & \gamma-\frac{v_1}{L} & 0 & 0 & -\Omega_1 A_0 \\ 0 & -\Omega_1 A_2 & 0 & \gamma^*-\frac{v_1}{L} & -\Omega_1 A_0^* & 0 \\ -\Omega_2 A_1^* & 0 & 0 & -\Omega_2 A_0 & \gamma+\frac{\Gamma}{2}+i\sigma|A_2|^2 & 0 \\ 0 & -\Omega_1 A_1 & -\Omega_2 A_0^* & 0 & 0 & \gamma^*+\frac{\Gamma}{2}-i\sigma|A_2|^2 \end{pmatrix} \begin{pmatrix} \delta a_0 \\ \delta a_0^* \\ \delta a_1 \\ \delta a_1^* \\ \delta a_2 \\ \delta a_2^* \end{pmatrix} = 0, \tag{27}$$

which will posses nontrivial solutions only if its determinant equals zero, which gives:

$$\begin{vmatrix} (\gamma+\frac{v_0}{L})(\gamma^*+\frac{v_0}{L}) & \Omega_0^2|A_2|^2 & \Omega_0^2|A_1|^2 \\ \Omega_1^2|A_2|^2 & (\gamma-\frac{v_1}{L})(\gamma^*-\frac{v_1}{L}) & -\Omega_1^2|A_0|^2 \\ \Omega_2^2|A_1|^2 & -\Omega_2^2|A_0|^2 & (\gamma+\frac{\Gamma}{2}+i\sigma|A_2|^2)(\gamma^*+\frac{\Gamma}{2}-i\sigma|A_2|^2) \end{vmatrix} = 0. \tag{28}$$

The aim of this analysis is to solve the equation (28) for its eigenvalue γ, and then to examine conditions for which $\mathrm{Re}\{\gamma\}$ changes its sign. i.e. to find critical conditions which produce γ=0. So, inserting this value for γ into (28), one obtains:

$$\begin{vmatrix} \frac{v_0^2}{L^2} & \Omega_0^2|A_2|^2 & \Omega_0^2|A_1|^2 \\ \Omega_1^2|A_2|^2 & \frac{v_1^2}{L^2} & -\Omega_1^2|A_0|^2 \\ \Omega_2^2|A_1|^2 & -\Omega_2^2|A_0|^2 & \frac{\Gamma^2}{4}+\sigma^2|A_2|^4 \end{vmatrix} = 0. \tag{29}$$

Development of the latter determinant leads to the equation:

$$\frac{v_0^2 v_1^2}{L^4}\frac{|A_0|^2|A_1|^2}{|A_2|^2} - 3\Omega_0^2\Omega_1^2|A_0|^2|A_1|^2|A_2|^2 - \frac{1}{L^2}\left(v_0^2\Omega_1^2|A_0|^4 + v_1^2\Omega_0^2|A_1|^4\right) = 0. \tag{30}$$

Note that $|A_2|^2$ is related to $|A_0|^2$ and $|A_1|^2$ through the relation:

$$\left(\frac{\Gamma^2}{4} + \sigma^2|A_2|^4\right)|A_2|^2 = \Omega_2^2\,|A_0|^2|A_1|^2, \tag{31}$$

following from (21).

Let us consider solutions of the equation (30) in the point x=0, as we observe the backscattered radiation coming just from this point:

$$|A_0(0)|^2 \to 1, \quad |A_1(0)|^2 \to \frac{v_0}{v_1}R.$$

If we introduce: $y = |A_2(0)|^2$, equations (30) and (31) become:

$$v_0^2\,v_1^2\,R - 3\,\Omega_0^2\,\Omega_1^2\,L^4 R\,y^2 - v_0\,v_1 L^2(\Omega_0^2\,R + \Omega_1^2)\,y = 0, \tag{32}$$

$$\sigma^2 y^3 + \frac{\Gamma^2}{4}\,y - \frac{v_0\,\Omega_2^2}{v_1}\,R = 0. \tag{33}$$

The equation (32) can be solved in y, and the solution substituted into (33). In this way, the solution of the latter equation Γ_{cr} is expressed in terms of n_0/n_{cr}, β_0, L and R. However, we note that stationary reflectivity R appears to depend on the pump strength β_0 and plasma length L; so, Γ_{cr} is a function of plasma density, length and pump strength.

Let us now consider the mentioned relation between β_0 and R. If we assume that the NLFS is still small at the onset of nonstationarity, the algebraic equation (21) produces the approximate expression:

$$A_2 = \frac{2\,\Omega_2}{\Gamma}\left(1 - i\,\frac{8\,\sigma\,\Omega_2^2}{\Gamma^3}\,|A_0|^2\,|A_1|^2\right)A_0\,A_1^*. \tag{34}$$

Substitution of (34) into (20a) and (20b) leads to the following equations:

$$\begin{aligned} v_0 A_0' &= -\frac{2\,\Omega_0\,\Omega_2}{\Gamma}\left(1 - i\,\frac{8\,\sigma\,\Omega_2^2}{\Gamma^3}\,|A_0|^2\,|A_1|^2\right)A_0\,|A_1|^2, \\ v_1 A_1' &= -\frac{2\,\Omega_1\,\Omega_2}{\Gamma}\left(1 - i\,\frac{8\,\sigma\,\Omega_2^2}{\Gamma^3}\,|A_0|^2\,|A_1|^2\right)|A_0|^2 A_1, \end{aligned} \tag{5}$$

which, after elementary transformation, produce:

$$\begin{aligned} \frac{d}{dx}|A_0|^2 &= -\frac{4\,\Omega_0\,\Omega_2}{v_0\Gamma}\,|A_0|^2\,|A_1|^2, \\ \frac{d}{dx}|A_1|^2 &= -\frac{4\,\Omega_1\,\Omega_2}{v_1\Gamma}\,|A_0|^2\,|A_1|^2. \end{aligned} \tag{36}$$

At this point, it is convenient to make use of the Mainly–Rowe relation resulting from the equations (36):

$$\frac{d}{dx}\frac{v_0}{\Omega_0}|A_0|^2 - \frac{v_1}{\Omega_1}|A_1|^2 = 0. \tag{37}$$

Referring to the entrance point (x=0), we obtain the value of the constant function in (37), with help of (18):

$$\frac{v_0}{\Omega_0}|A_0|^2 - \frac{v_1}{\Omega_1}|A_1|^2 = \text{const.} = \frac{v_0}{\Omega_0}(1-r), \tag{38}$$

where we introduced:

$$r = \frac{\Omega_0}{\Omega_1}R. \tag{39}$$

The quantity r is a normalized (relative) reflectivity, whose maximum value in the stationary state equals unity. The latter fact has, as a consequence: $R_{max} = \Omega_1/\Omega_0 = \omega_1/\omega_0 = 1-\alpha$.

The system (36) can be solved to give:

$$|A_0(x)|^2 = \frac{1-r}{1-r\,e^{-\chi(1-r)x}}, \quad |A_1(x)|^2 = \frac{v_0\Omega_1}{v_1\Omega_0}\frac{r(1-r)}{e^{\chi(1-r)x}-r}, \tag{40}$$

where:

$$\eta = \frac{v_0\Omega_1}{v_1\Omega_0}, \quad \chi = \frac{4\Omega_1\Omega_2}{v_1\Gamma}. \tag{41}$$

The nonlinear perturbations in the equations (36) bring imaginary corrections into expressions for A_0 and A_1, which are not essential, but we give them for completeness:

$$A_{0,1} = |A_{0,1}|\,e^{i\varphi_{0,1}}, \tag{42}$$

where $|A_0|$ and $|A_1|$ follow from (40) and phases φ_0 and φ_1 are obtained by substitution of (42) into the equations (36) and linearization of the latter:

$$\varphi_0 = -\frac{2\sigma\Omega_2^2}{\Gamma^3}|A_1|^4, \quad \varphi_1 = \frac{2\sigma\Omega_2^2}{\Gamma^3}|A_0|^4. \tag{43}$$

In order to check if we are on the right path, we plot down the steady–state spatial profiles of the pump and backscattered amplitudes $|A_0(x)|$ and $|A_1(x)|$, resulting from the simulation of the equations (8) and the approximate approach leading to the expressions (40). This is given in the Fig. 3, for the case of parameters of Fig. 1. A high degree of accordance between the two approaches encourages us to proceed searching for the estimation of the critical conditions corresponding to the bifurcation from a steady–state to an oscillatory state which is an indication of irregular, essentially nonstationary regimes.

The reflectivity R, or r, appearing above is still an undetermined quantity. It can be evaluated by comparing the expressions (40) to the boundary conditions (22):

$$\frac{\eta\,r(1-r)}{e^{\chi(1-r)L}-r} = \varepsilon^2. \tag{44}$$

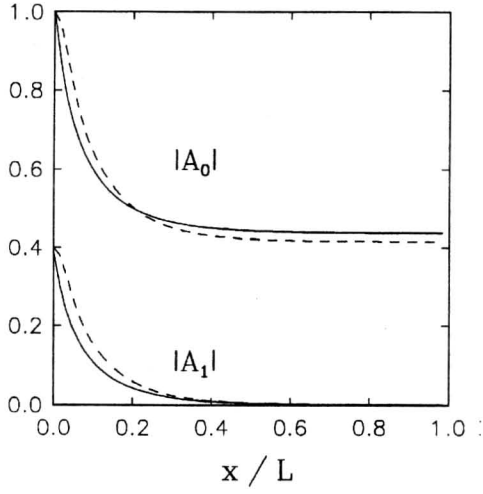

Fig. 3. Comparison of spatial dependances of the pump and backscattered wave amplitudes in the saturated steady state, obtained by direct simulation (dashed lines) and approximate approach of section 4. (solid lines), for the parameters of Fig. 2a.

The system of equations (32), (33) and (44) appears to be the crucial result of the present paper. It enables one to determine, for any set of input parameters, what kind of saturated SRBS behaviour will be exhibited. This system of two algebraic and one transcendental equations can not be solved in a close form, though it is numerically solvable. We seek for a solution such that y, R and Γ^2 are positive values.

Solving (12) in y gives:

$$y = \frac{v_0 v_1}{\Omega_0 \Omega_1 L^2} \frac{\sqrt{1+14r^2+r^4} - (1+r^2)}{r}. \tag{45}$$

Of particular interest to us is a case of r still well under the order of unity, for which:

$$y \approx \frac{v_0 v_1}{\Omega_0 \Omega_1 L^2} r, \tag{46}$$

which follows from (45) in the limit $r \ll 1$. As for the normalized reflectivity r appearing in the above expressions, it can be approximately evaluated from (44), assuming $r \ll 1$:

$$r \approx \frac{\varepsilon^2}{\eta} \exp(\chi L). \tag{47}$$

Note that r depends on β_0 and Γ through the parameter χ, given by (41). Thus, we substitute (46) and (47) into (33) to obtain the final relation connecting between system parameters: β_0, Γ_{cr}, L and n_0/n_{cr}:

$$A^2 l^2 \beta_0^2 - \nu^2 = \frac{B}{l^4} \exp\left(C \frac{l\beta_0^2}{\nu}\right), \tag{48}$$

where

$$l \equiv \frac{L\omega_0}{C}, \quad \nu \equiv \frac{\Gamma}{\omega_{pe}}, \tag{49}$$

and constants A, B and C depend on the rest of parameters:

$$A = \frac{\left(\sqrt{1-\alpha^2}+\sqrt{1-2\alpha}\right)}{8\alpha\sqrt{1-2\alpha}}, \quad B = \frac{1024\left(\frac{\sigma}{\omega_{pe}}\right)^2(1-2\alpha)^2\varepsilon^4}{\alpha^8(1-\alpha)^4}, \tag{50}$$
$$C = \frac{\left(\sqrt{1-\alpha^2}+\sqrt{1-2\alpha}\right)}{2\sqrt{1-2\alpha}}.$$

It can be readily estimated that the term ν^2 in the equation (48) is small in relation to the preceding one, so, we obtain finally:

$$\nu_{cr} = \frac{C\beta_0^2 l}{\ln\left(\frac{A^2\beta_0^2 l^6}{B}\right)}. \tag{51}$$

Thus, for the parameters applied in simulations of the Fig. 1 series (β_0=0.03, α=$\sqrt{0.1}$, β_T=$1/\sqrt{511}$, L=$100c/\omega_0$) we obtain the critical damping value Γ_{cr}=$0.004\,\omega_{pe}$ corresponding to the reflectivity $R \approx 2.6\times10^{-2}$. In a similar way, numerical solution of the mentioned equations for parameters of Fig. 2 (β_0=0.1) gives: Γ_{cr}=$0.042\,\omega_{pe}$, R=0.365. These results are quite in accordance with the results of direct simulation presented in these figures.

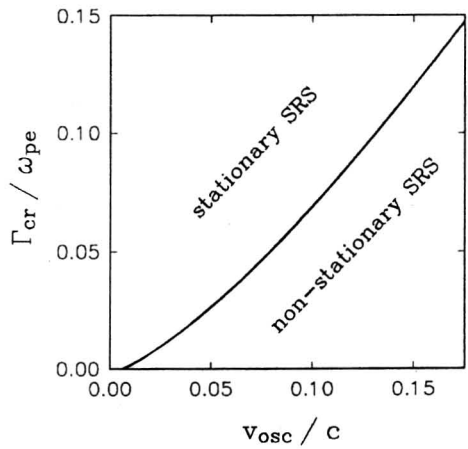

Fig. 4. Bifurcation diagram that enables the prediction of the saturated behaviour of the SRBS for different combinations of values of β_0 and Γ, and for: n_e=$0.1n_{cr}$, L=$100c/\omega_0$, κT_e=$1keV$.

The relation (51) determines Γ_{cr} in terms of pump strength β_0, plasma length l and density $\alpha=\sqrt{n_0/n_{cr}}$ on a bifurcation line between stationary and nonstationary saturated nonlinear regimes of the SRBS. The bifurcation diagram in Fig. 4 illustrates the fact that the increase in β_0 and decrease in Γ make the system transit from a steady–state to a nonstationary saturation. The role of the other parameters is exhibited in Figs. 5 and 6, from which it is seen that the shortening of the plasma has the same effect as the increase in damping coefficient. Similarly, for moderate densities ($n_0/n_{cr} < .0.14$), for which the above approximations are valid, an increase in the density stabilizes the process, i.e. leads this process into the stationary regime.

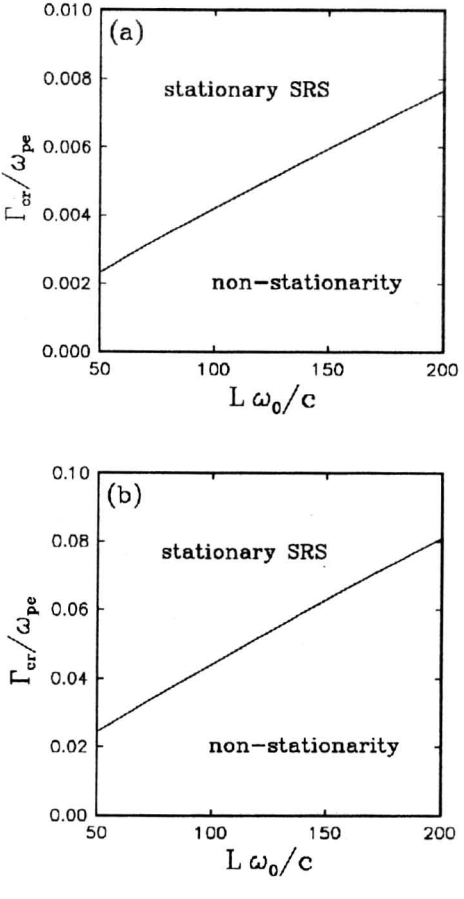

Fig. 5. Bifurcation diagram $L - \Gamma$ for $n_e=0.1n_{cr}$, $\kappa T_e=1keV$, and β_0: a) 0.03, b) 0.1.

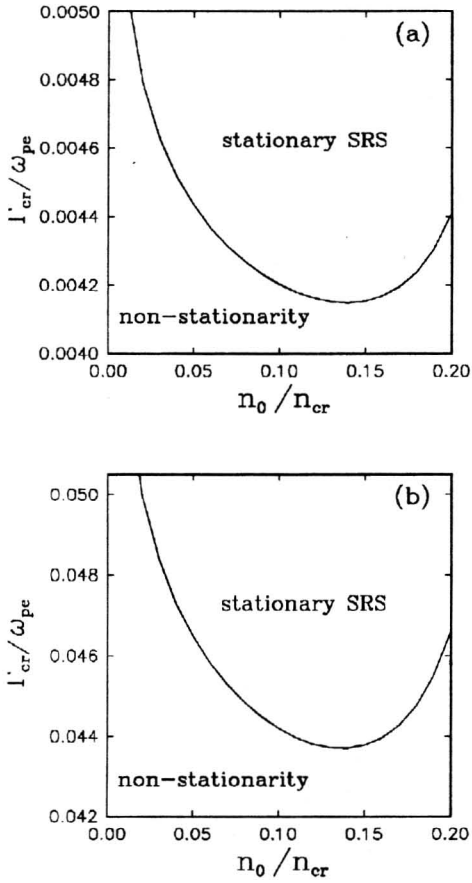

Fig. 6. Bifurcation diagram n_0 – Γ for $L=100c/\omega_0$, $\kappa T_e=1keV$, and β_0: a) 0.03, b) 0.1.

5. Conclusion

The present paper deals with the asymptotic behaviour of SRBS in a homogeneous plasma layer with specified parameters. The system of first–order partial differential equations describing the spatio–temporal evolution of the slowly–varying wave amplitudes was simulated for different values of pump strength and wave damping. The crucial role in the nonlinear development of the Raman instability is played by a self–modal cubic nonlinearity in the form of NLFS in the EPW equation. The numerical simulation of the SRBS equations revealed a tendency of the system to transit from a stable, stationary, nonlinear saturated state to a periodic, aperiodic, or chaotic–like regimes, when the EPW damping rate was gradually reduced. Then, an analytical procedure was applied in order to enlighten and confirm such a behaviour. By linearizing the wave functions around the point

of the onset of nonstationarity, the relations were derived that connect quantitatively the essential parameters of the system around the bifurcation surface, and which enable one to predict a type of asymptotic SRBS behaviour for given laser and plasma parameters. The agreement between the results of numerical and analytical treatments was underlined as well.

References:

[1] W.L. Kruer, *"The Physics of Laser Plasma Interactions"* (Addisson–Wesley, New York, 1988), and references therein.
[2] D.W. Forslund, J.M. Kindel, E. Lindman, *Phys. Fluids* **18** (1975) 1002.
[3] R.P. Drake, S.H. Batha, *Phys. Fluids*, **B3** (1991) 2936.
[4] C.J. McKinstrie, A. Simon, *Phys. Fluids B* **29** (1986) 1959.
[5] J.A. Heikkinen, S.J. Karttunen, *Phys. Fluids* **29** (1986) 1291.
[6] T. Kolber, W. Rozmus, V.T. Tikhonchuk, *Phys. Fluids B* **5** (1993) 138; ibid. *Phys. Plasmas* **2** (1995) 256.
[7] B. Bezzerides, D.F. DuBois, H.A. Rose, *Phys. Rev. Lett.* **70** (1993) 2569.
[8] D.M. Villeneuve, K.L. Baker, R.P. Drake, B. Sleaford, B. LaFontaine, K. Estabrook, M.K. Prasad, *Phys. Rev. Lett.* **71** (1993) 368.
[9] C.B.Darrow, C. Coverdale, M.D. Perry, W.B. Mori, C. Clayton, K. Marsh, C. Joshi, *Phys. Rev. Lett.* **69** (1992) 442.
[10] H. Baldis, D.M. Villeneuve, C. Labaune, D. Pesme, W. Rozmus, W.L. Kruer, P.E. Young, *Phys. Fluids B* **3** (1991) 2341.
[11] G. Bonnaud, D. Pesme, R. Pellat, *Phys. Fluids B* **2** (1990) 1618; *ibid.* **4** (1992) 423.
[12] R. Bingham, *Physica Scripta* **T30** (1990) 24.
[13] F.F. Chen, *Physica Scripta*, **T30** (1990) 14.
[14] M.M. Škoric, M.S. Jovanović, in *"Laser Interaction and Related Plasma Phenomena" vol. 11*, ed. by G.H. Miley (AIP, New York, 1994) p. 380.
[15] M.S. Jovanović, Ph.D. Thesis, University of Belgrade (1994).
[16] R.R.E. Salomaa, S.J. Karttunen, *Physica Scripta* **33** (1986) 370.
[17] T.W. Johnston, P. Bertrand, A. Ghizzo, M. Shoucri, E. Fijalkow, M.R. Feix, *Phys. Fluids* **B4** (1992) 2523.
[18] D.L. Book, *"NRL Plasma Formulary"* (Naval Research Laboratory, Washington, 1990) p. 51.
[19] H.A. Baldis, E.M. Campbell, W.L. Kruer, in *"Handbook of Plasma Physics" vol. 3: "Physics of Laser Plasma"*, ed. by A.M. Rubenchik and S. Witkowski (Elsevier Science Publishers B.V., Amsterdam, 1991) p. 361.
[20] P. Bergé, Y. Pomeau, C. Vidal, *"Order within Chaos"* (Hermann, Paris, 1984) p. 223.
[21] M.M. Škorić, M.S. Jovanović, M.R. Rajković, in *"Dynamical Systems and Chaos"*, ed. by Y. Aizawa, S. Saito and K. Shiraiwa (World Scientific, Singapore, 1995) p. 165.
[22] M.M. Škorić, M.S. Jovanović, M.R. Rajković, to be published in *Phys. Rev. E.*

UTICAJ AMORTIZACIJE TALASA NA PONAŠANJE STIMULISANOG RAMANOVOG RASEJANJA U HOMOGENOJ PLAZMI

Moma S. Jovanović* i Miloš M. Škorić**

Sadržaj: U radu se razmatra problem (ne)stacionarnosti nelinearnog zasićenog režima stimulisanog Ramanovog rasejanja unazad u homogenom sloju plazme. Jednačine za sporo promenljive talasne obvojnice, uz uključenu amortizaciju i nelinearni frekventni pomak, rešavane su numerički i analitički. Pokazano je da promena koeficijenta amortizacije vodi sistem kroz različite dinamičke režime, od stacionarnog do haotičnog. Izvedene su i diskutovane kvantitativne relacije koje omogućuju predviđanje tipa asimptotskog ponašanja Ramanove nestabilnosti u plazmi.